Scanning tunneling microscopy of doping and compositional III–V homo- and heterostructures

S. Gwo, K.-J. Chao, A. R. Smith, and C. K. Shih
Department of Physics, University of Texas, Austin, Texas 78712

K. Sadra and B. G. Streetman
Microelectronics Research Center and Department of Electrical and Computer Engineering, University of Texas, Austin, Texas 78712

(Received 19 February 1993; accepted 1 April 1993)

Scanning tunneling microscopy (STM) was used to study the (110) cross-sectional surfaces of molecular-beam epitaxially grown III–V homo- and heterostructures, which include GaAs multiple *p–n* junctions, (InGa)As/GaAs strained-layer multiple quantum wells, and (AlGa)As/GaAs heterojunctions. Both doping and compositional effects can be resolved by the topographic contrasts of constant-current STM images. The samples were prepared by either cleaving in ultrahigh vacuum or cleaving *ex situ* followed by sulfide $[(NH_4)_2S]$ passivation. Sulfide passivated samples have been found to be advantageous for the measurements of scanning tunneling spectroscopy.

I. INTRODUCTION

The advances of semiconductor growth technology have made possible the realization of highly sophisticated nanometer-size heterostructure devices. However, the quest for fully understanding the properties of semiconductor heterostructures has never come to an end. Compared with the conventional techniques such as photoluminescence, photoemission, and *C–V* measurements, scanning tunneling microscopy and spectroscopy (STM/S) have unprecedented resolution for mapping out the spatial variation of electronic properties. Thus, it is an ideal tool for studying heterostructures provided that (1) one can prepare a cross-sectional surface which exposes the junctions, and (2) the study performed on such a surface will not obscure the interpretation of the bulk electronic properties. As a result, a large number of cross-sectional STM/S studies have been performed on III–V compound semiconductors. This is because the junctions are automatically exposed by cleaving the sample to prepare a (110) cross-sectional surface, and the dangling bond states of the cleaved (110) surface are outside the bulk band gap. However, despite such promising potential, the progress of STM/S of semiconductor heterostructures has been slow due to some technical difficulties. The first obvious difficulty of this approach is the positioning of the tunneling tip within the epilayer region which usually has a length scale of less than a micron.

Salemink and co-workers obtained the first atomic images of (AlGa)As/GaAs heterojunctions by using cross-sectional STM.[1,2] They also reported scanning tunneling spectroscopy results across the heterojunctions with nanometer resolution. In their studies, an ultrahigh vacuum (UHV) scanning electron microscope (SEM) was employed to help locate the STM tip within the epilayer region. However, due to the difficulty of maintaining sample surface cleanliness and the additional complexity of tip-induced band bending on unpinned sample surfaces, the resulting band offsets measured by tunneling spectroscopy did not directly reflect the properties of the buried bulk heterointerface.[1] Other efforts to perform cross-sectional STM/S investigations of semiconductor junctions have also been made such as studies of Si and GaAs *p–n* junctions,[3–12] $In_{0.47}Ga_{0.53}As/InP$ multiple quantum wells (MQWs),[13] P_2S_5 passivated (AlGa)As/GaAs MQWs,[14] and HF passivated $Si/Si_{0.76}Ge_{0.24}$ superlattices.[15] It should be mentioned that most of these studies, including ours, did not employ an UHV SEM. Instead, several versions of edge finding techniques were used to locate the tip within the epilayer region.

In this article, we report STM studies of various multilayered structures including GaAs multiple *p–n* junctions, $In_{0.2}Ga_{0.8}As/GaAs$ strained-layer MQWs, and $Al_{0.3}Ga_{0.7}As/GaAs$ heterojunctions. Cross sections of samples were prepared by two methods: (1) *in situ* cleaving in an UHV chamber, and (2) *ex situ* cleaving followed by chemical passivation. We have found that for chemically passivated samples, the difficulty of maintaining the cleanliness of sample surfaces is overcome, especially in the case of (AlGa)As. Moreover, due to the uniform Fermi level pinning at the passivated surface, the tip-induced band bending effect is minimized, resulting in very reproducible and stable tunneling spectroscopy results.

II. EXPERIMENTAL

Our experiments were performed in an UHV STM system equipped with a dual-axis sample translation stage and a sample load lock. The III–V doping and compositional structures were grown on (001) substrates (*n*-type, 1×10^{18} cm^{-3}) using molecular-beam epitaxy (MBE). Si and Be were used as dopants (doping concentrations in our samples varied from 5×10^{17} cm^{-3} to 2×10^{18} cm^{-3}). The multilayered structures were grown at 600 °C for doping homojunctions and 620 °C for $Al_{0.3}Ga_{0.7}As/GaAs$ heterojunctions. Samples were prepared for cleaving by cutting wafers into rectangular pieces 3×10 mm^2 and scribing notches on top of the epilayer with a diamond pen.

 ©1993 American Vacuum Society

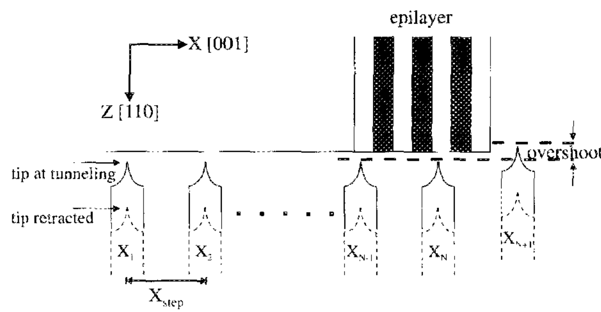

FIG. 1. A schematic diagram of the edge-finding procedure. First, we start with the tip at a position within 10–20 μm from the edge, which is easily achievable using an optical microscope. Second, we bring the tip in the tunneling regime. Finally, we iterate the process of recording the tip position, withdrawing the tip, stepping the sample laterally, and reapproaching the tip. In this algorithm, X_{step} is typically 2000–3000 Å. The sample edge can be identified when the tip position extends beyond the previous position in the tunneling regime.

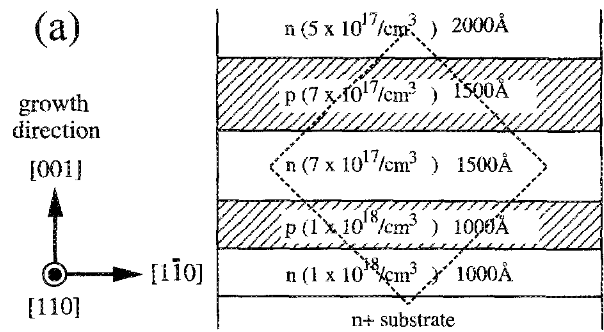

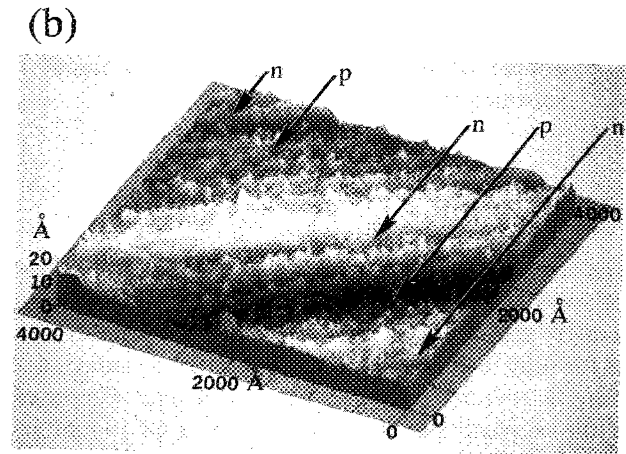

FIG. 2. (a) The structure of GaAs multiple *p–n* junctions grown by MBE. The area enclosed by the dashed line corresponds to the STM image. (b) A 3D perspective view of the STM image of the GaAs multiple *p–n* junctions acquired with a sample bias of −2.9 V and a tunneling current of 0.8 nA. The scanning area is 4000 Å×4000 Å.

In situ cleaving was performed by pushing on the sample along the [00$\bar{1}$] direction. The typical UHV pressure was 6×10^{-11} Torr or less. Chemically passivated samples were cleaved *ex situ* and passivated in an ammonium sulfide [$(NH_4)_2S$] solution at room temperature for 5–20 min [in our studies, cleaving inside the $(NH_4)_2S$ solution made no significant difference]. After rinsing in de-ionized water and blowing dry with nitrogen gas, samples were immediately transferred into the UHV chamber through a load lock for STM/S measurements. The tungsten tunneling tips were made by electrochemical etching followed by *in situ* cleaning using the field emission method on separate clean substrates.

In our experiments, to position the tunneling tip within the epilayer region, we used the following edge-finding algorithm: as shown in Fig. 1, the tip was first brought into tunneling in the vicinity of the epilayer region. Subsequent iteration of recording the tip position, withdrawing the tip, stepping the sample laterally, and reapproaching the tip allowed us to find the edge of the sample surface. At the end of the edge-finding procedure, the tip was stepped back into the epilayer. The success of this method depends primarily upon two things. First, the sample must be extremely flat all the way up to the edge. Second, a two-dimensional sample mover which is free of backlash and crosstalk is necessary. Without meeting these requirements,[16] it will be very difficult to avoid crashing the tip.

III. RESULTS AND DISCUSSION

STM results reported here primarily concentrate on the delineation of junctions in epilayer regions. Detailed spectroscopy results will be reported elsewhere.[17] In our studies, the assignments of different junctions are primarily based on the comparison of topographical contrast features with the MBE growth structures.

A. UHV cleaved samples

Studies on two types of UHV cleaved samples will be reported here: GaAs multiple *p–n* junctions and $In_{0.2}Ga_{0.8}As$/GaAs strained-layer MQWs. Shown in Figs. 2(a) and 2(b) are the growth structure and a perspective view of a constant-current STM image acquired at a sample bias voltage of −2.9 V. The dashed box shown in Fig. 2(a) corresponds to the scanning area shown in Fig. 2(b). The constant-current STM images of GaAs multiple *p–n* junctions show pronounced topographic contrast (ranging from 2.5 to 5 Å), independent of bias polarities, between *n* and *p* layers due solely to the electronic effect.[10,11] Detailed analysis of this result has been reported earlier and will not be repeated here.

The second sample system to be reported here is the $In_{0.2}Ga_{0.8}As$/GaAs strained-layer MQW system [the structure is shown in Fig. 3(a)]. Fig. 3(b) is a constant-current STM image acquired at a sample bias voltage of −1.97 V. The topographical features in Fig. 3(b) show a general consistency with the MBE growth structure. However, one can also clearly see that the interfaces do not appear to be abrupt in the STM image. There are a few possibilities for

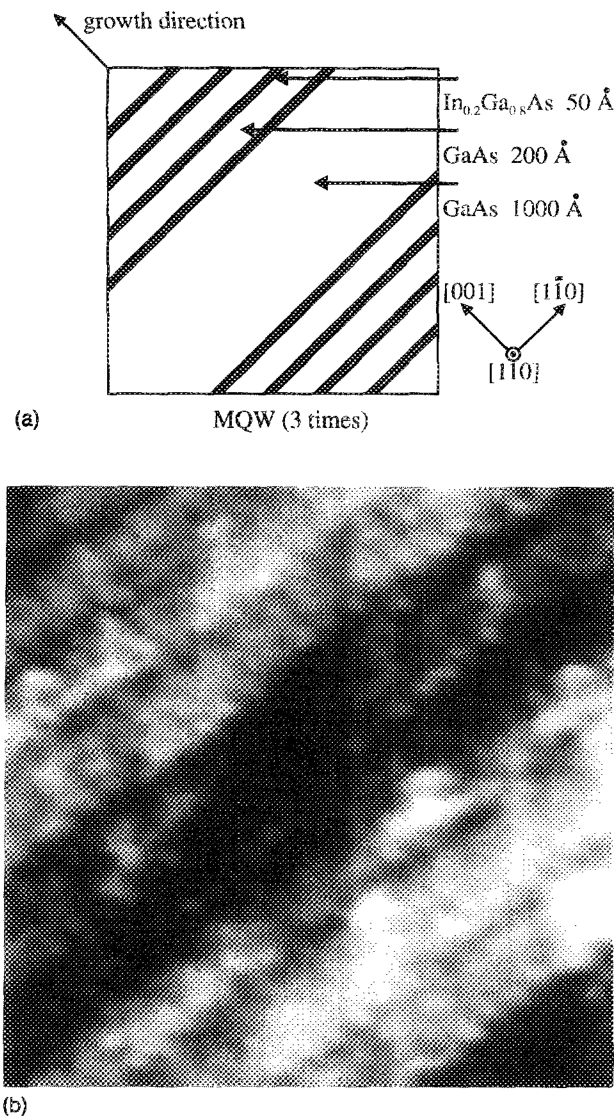

FIG. 3. (a) The structure of $In_{0.2}Ga_{0.8}As/GaAs$ strained-layer multiple quantum wells grown by MBE (*n*-type Si doped, 1×10^{18} cm^{-3}). (b) A STM image of the (InGa)As/GaAs strained-layer multiple quantum wells ($V_s=-1.97$ V, $I_t=0.23$ nA). The image is shown in a grey scale over a range of 1.5 Å. The scanning area is 2500 Å×2500 Å.

this nonabruptness of the interfaces observed in the STM. The first possibility is that this nonabruptness is due to the cleaving process which causes additional strain relaxation at the interface region near the vacuum/solid junction. The second possibility is that this nonabruptness is a true interface property of our sample, resulting from the formation of three-dimensional (3D) islands during the epilayer growth.

While the nonabruptness can be easily seen in the STM image, we have faced difficulties in the assignment of the (InGa)As and GaAs regions. As one can see, the STM image shows wide bright bands with narrow dark regions between them. Since the growth thickness of the (InGa)As layer is clearly smaller as shown in the growth structure, one might conclude that the dark bands correspond to the (InGa)As regions. However, the number of dark bands would then not be consistent with the number of growth layers of (InGa)As (three as compared with four in the upper left of the image). Furthermore, we also have difficulty explaining why the GaAs buffer layer between the MQWs appears to be dark. In addition, the width of the center dark band is smaller than the thickness of the GaAs buffer layer. The alternative interpretation is that the centers of the bright bands correspond to the (InGa)As regions which have narrower band gaps than the GaAs regions, and it is the electronic effect which causes the spreading of the bright regions. This alternative interpretation would be consistent with the reported work on (InGa)As/InP MQWs (Ref. 13) where the bright regions were assigned to be the narrower gap regions of (InGa)As. However, we still need to explore which electronic effects are responsible for the observed spreading.

We should mention that the success rate for obtaining images with topographic features consistent with the growth parameters is low for UHV-cleaved cross-sectional surfaces. We believe that the problem lies primarily in the difficulty of obtaining a very flat epilayer region during the *in situ* cleaving process. For example, we often observe very long and straight step edges running across the whole scanning area, thus obscuring our ability to delineate the junctions. In these cases, the assignments will have to rely on extensive spectroscopy studies.

B. Sulfide passivated samples

The low success rate of preparing cross-sectional surfaces by the use of *in situ* cleaving has motivated us to seek an alternative approach. We have found that *ex situ* cleaving followed by chemical passivation using a $(NH_4)_2S$ solution[18–20] yields dramatic results. First of all, the *ex situ* method provides better control of the cleavage process. Furthermore, one can then select the best-cleaved samples before loading into the UHV chamber. Apart from this, the chemical passivation method offers two additional advantages. The first is that the passivated surface prevents adsorption of oxygen contaminants. This is particularly important for studies of (AlGa)As systems since oxygen contamination is a very severe problem.[1] The second is that the chemical passivation process results in a uniform surface Fermi-level pinning. Thus, the tip-induced band bending effect is substantially reduced, allowing us to obtain very reproducible and stable tunneling spectra. A similar Fermi level pinning effect has been reported by Feenstra *et al.* on highly stepped surfaces of GaAs doping superlattices.[11]

In Fig. 4(a), we show the structure grown by MBE for the studies of $Al_{0.3}Ga_{0.7}As/GaAs$ heterojunctions. The structure was designed in such a way that four types (*n–n*, *n–p*, *p–n*, and *p–p*) of heterojunctions could be studied and compared. Figure 4(b) is the corresponding STM image of an area 7000 Å×7000 Å, acquired at a sample bias of −2.35 V. Since the GaAs buffer layer is included in this image, it serves as a marker to facilitate the assignment of regions with different doping and composition. Also shown in Fig. 4(b) is a cross-sectional profile across the heterojunctions of the STM image. Because the scanning direction (*x* direction) was aligned with the [00$\bar{1}$] direction, the profile is obtained by simply averaging line scans along the

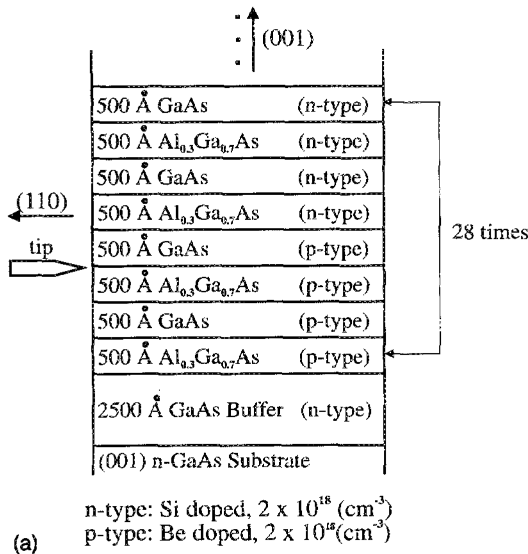

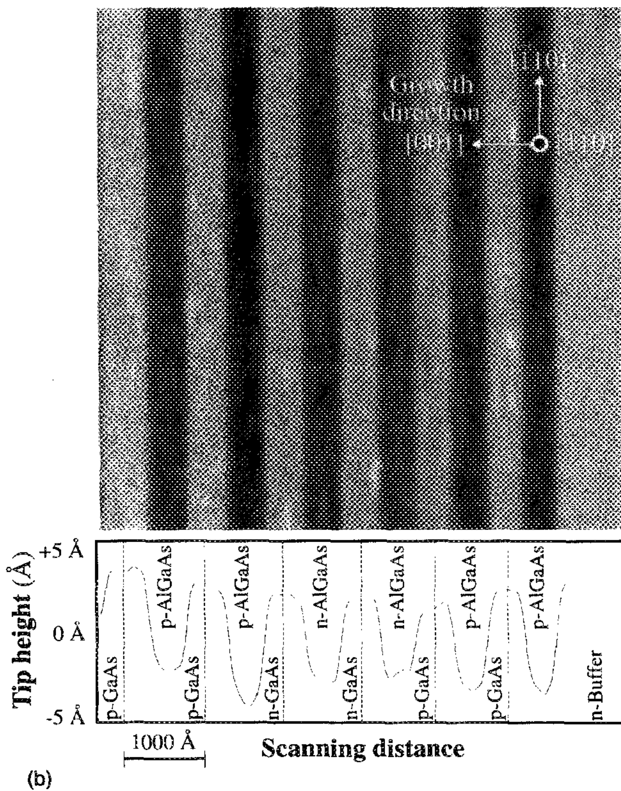

FIG. 4. (a) The structure of $Al_{0.3}Ga_{0.7}As/GaAs$ heterojunctions grown by MBE. (b) A 7000 Å×7000 Å STM image of $Al_{0.3}Ga_{0.7}As/GaAs$ heterojunctions. This sample was cleaved *ex situ* and chemically passivated by ammonium sulfide immediately. This image was acquired in UHV with a sample bias of −2.35 V and a tunneling current of 0.3 nA. The *n*-GaAs buffer layer can be seen on the right-hand side of the image. Below this image is the cross-sectional profile of the heterojunctions.

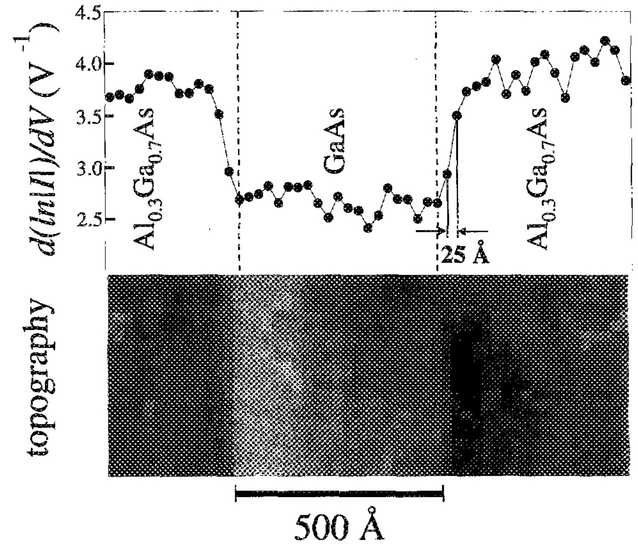

FIG. 5. A portion of a 64×64 pixel STM image in which tunneling I–V spectra were taken at every pixel in the image. The upper part of the figure is the plot of normalized conductivity $d(\ln|I|)/dV$ (derived from tunneling I–V spectra) vs position at a sample bias of −1.7 V. Because $d(\ln|I|)/dV$ is given to lowest order by $1/(V-V_0)$ where V_0 is the position of the band edge, the normalized conductivity is larger in the regions of $Al_{0.3}Ga_{0.7}As$ due to the valence band offset.

[1$\bar{1}$0] direction (y direction). This cross-sectional profile shows that (AlGa)As regions appear deeper than GaAs regions by about 5 Å. Additionally, the two p-type (AlGa)As layers adjacent to the n-type GaAs layer appear to be deeper than the two n-type (AlGa)As layers. We attribute this latter feature to be solely an electronic effect. The generally deeper appearance of the (AlGa)As regions is most likely due to a combination of the electronic effect from the valence band offset (VBO) and a true difference in surface height. Indeed, it has been shown that sulfide solutions have a greater etching rate on (AlGa)As than GaAs.[14] Although we have not observed the rectangular atomic unit cell of the UHV-cleaved (110) surface in our STM images of these sulfide passivated surfaces, the measured root-mean-square (rms) roughness in the substrate region of such a sulfide passivated surface was measured to be less than 0.5 Å, indicating an atomically flat surface.

As mentioned above, tunneling spectroscopy performed on the sulfide passivated surface is extremely stable. Shown in Fig. 5 is a 53×21 pixel STM image in which I–V tunneling spectra were taken at every pixel in the image. Since the electronic structure along the [1$\bar{1}$0] direction is uniform, spectra are averaged along this direction to improve the signal to noise ratio. In order to analyze the resulting data, we consider the technique used by Feenstra *et al.*[11] In performing STM/S studies of GaAs p–n superlattices, they found that the conductivity image at constant current and constant voltage could be used to delineate the electronic junctions. They argued that to a zeroth order approximation $dI/dV \sim I/(V-V_0)$ where V_0 represents the location of the band edge. Thus, if the sample bias is closer to the band edge, $d\ln|I|/dV$ will be larger. Following their argument, we have plotted the normalized conductivity $d(\ln|I|)/dV$ versus position for various bias voltages. Indeed, one observes that $d(\ln|I|)/dV$ at a constant negative sample bias is much larger in the (AlGa)As region, indicating the effect of the VBO. One can take this argument one step further by estimating the band offset from this conductivity profile using the zeroth order approximation $d(\ln|I|)/dV \sim I/(V-V_0)$. From this conductivity

profile, we estimate the valence band offset to be about 0.16±0.05 eV. This value is considerably smaller than that reported by Salemink *et al.*[1] We believe that this difference is due to the absence of the tip-induced band bending effect in our measurements. We should mention that this is only an estimation based on a zeroth order approximation. A much more detailed analysis, including the conduction band offset, will be reported elsewhere.[17]

IV. SUMMARY

Cross sections of MBE grown doping and compositional homo- and heterostructures were investigated with an UHV STM. In our studies, both UHV cleaving and *ex situ* cleaving followed by chemical passivation were used to prepare the sample cross sections. All studies were conducted in an UHV environment. For sulfide passivated samples, we have found that the difficulty of maintaining the cleanliness of sample surfaces, especially in the case of (AlGa)As, is overcome. In addition, the tip-induced band bending effect is minimized on sulfide passivated surfaces, resulting in very reproducible and stable tunneling spectroscopy results.

ACKNOWLEDGMENTS

This work was supported by the Texas Advanced Research Program, the Joint Services Electronics Program (Contract No. AFOSR F49620-92-C-0027), and the Science and Technology Center Program of National Science Foundation (NSF) (Grant No. CHE8920120). We thank S. Wright for providing us the MBE grown $In_{0.2}Ga_{0.8}As$/GaAs sample. We also thank R. M. Feenstra and J. A. Dagata for useful discussions.

[1]O. Albrektsen, D. J. Arent, H. P. Meier, and H. W. M. Salemink, Appl. Phys. Lett. **57**, 31 (1990); H. W. M. Salemink and O. Albrektsen, J. Vac. Sci. Technol. B **9**, 779 (1991); H. W. M. Salemink, O. Albrektsen, and P. Koenraad, Phys. Rev. B **45**, 6946 (1992); H. W. M. Salemink and O. Albrektsen, J. Vac. Sci. Technol. B **10**, 1799 (1992).

[2]In the following experiments, electroluminescence associated with STM in (AlGa)As/GaAs heterostructures is used to image the energy profile of quantum wells: D. L. Abraham, V. Veider, Ch. Schönenberger, H. P. Meier, D. J. Arent, and S. F. Alvarado, Appl. Phys. Lett. **56**, 1564 (1990); S. F. Alvarado, Ph. Renaud, D. L. Abraham, Ch. Schönenberger, D. J. Arent, and H. P. Meier, J. Vac. Sci. Technol. B **9**, 409 (1991); Ph. Renaud and S. F. Alvarado, Phys. Rev. B **44**, 6340 (1991).

[3]P. Muralt, Appl. Phys. Lett. **49**, 1441 (1986).

[4]P. Muralt, H. Meier, D. W. Pohl, and H. W. M. Salemink, Appl. Phys. Lett. **50**, 1352 (1987).

[5]S. Hosaka, S. Hosoki, K. Takata, K. Horiuchi, and N. Natsuaki, Appl. Phys. Lett. **53**, 487 (1988).

[6]M. B. Johnson and J.-M. Halbout, J. Vac. Sci. Technol. B **10**, 508 (1992).

[7]S. Kodic, E. J. van Loenen, and A. J. Walker, Appl. Phys. Lett. **59**, 3154 (1991); IEEE Trans Electron Device Lett. **EDL-12**, 422 (1991); J. Vac. Sci. Technol. B **10**, 496 (1992).

[8]E. T. Yu, M. B. Johnson, and J.-M. Halbout, Appl. Phys. Lett. **61**, 201 (1992).

[9]R. Chapman, M. Kellam, S. Goodwin-Johansson, J. Russ, G. E. McGuire, and K. Kjoller, J. Vac. Sci. Technol. B **10**, 502 (1992).

[10]S. Gwo, A. R. Smith, C. K. Shih, K. Sadra, and B. G. Streetman, Appl. Phys. Lett. **61**, 1104 (1992).

[11]R. M. Feenstra, E. T. Yu, J. M. Woodall, P. D. Kirchner, C. L. Lin, and G. D. Pettit, Appl. Phys. Lett. **61**, 795 (1992); R. M. Feenstra, A. Vaterlaus, E. T. Yu, P. D. Kirchner, C. L. Lin, J. M. Woodall, and G. D. Pettit, *Proceedings of Physical Properties of Semiconductor Interfaces at Sub-Nanometer Scale*, 1992, edited by H. W. M. Salemink (Kluwer, Dordrecht, to be published).

[12]J. A. Dagata, W. Tseng, and R. M. Silver (in preparation).

[13]T. Kato, F. Osaka, and I. Tanaka, Jpn. J. Appl. Phys. **27**, L1193 (1988); T. Kato, F. Osaka, and I. Tanaka, *ibid.* **28**, 1050 (1989); T. Kato and F. Osaka, Jpn. J. Appl. Phys. **30**, L1586 (1991); T. Kato, F. Osaka, I. Tanaka, and S. Ohkouchi, J. Vac. Sci. Technol. B **9**, 1981 (1991); T. Kato and F. Osaka J. Appl. Phys. **72**, 5716 (1992).

[14]J. A. Dagata, W. Tseng, J. Bennett, J. Schneir, and H. H. Harary, Appl. Phys. Lett. **59**, 3288 (1991); Ultramicroscopy, **42**, 1288 (1992).

[15]E. T. Yu, J.-M. Halbout, A. R. Powell, and S. S. Iyer, Appl. Phys. Lett. **61**, 3166 (1992).

[16]A. R. Smith, S. Gwo, and C. K. Shih (in preparation).

[17]S. Gwo, K.-J. Chao, C. K. Shih, K. Sadra, and B. G. Streetman (in preparation).

[18]C. J. Sandroff, R. N. Nottenburg, J.-C. Biscoff, and R. Bhat, Appl. Phys. Lett. **51**, 33 (1987); R. N. Nottenburg, C. J. Sandroff, D. A. Humphrey, T. H. Hollenbeck, and R. Bhat, *ibid.* **52**, 218 (1988).

[19]M. R. Melloch, M. S. Carpenter, T. E. Dungan, D. Li, and N. Otsuka, Appl. Phys. Lett. **56**, 1064 (1990).

[20]Y. Nannichi, J.-F. Fan, H. Oigawa, and A. Koma, Jpn. J. Appl. Phys. **27**, L2367 (1988).